

Observation of a microwave bandgap in a one-dimensionally periodic low-pressure plasma structure

Kazunori Takahashi^{1,2,3} and Kazuaki Miyamoto²

¹Department of Electrical Engineering, Tohoku University, Sendai 980-8579, Japan

²Department of Electric Engineering and Computer Science, Iwate University, Morioka 020-8551, Japan

³Soft-Path Engineering Research Center, Iwate University, Morioka 020-8551, Japan

E-mail: kazunori@ecei.tohoku.ac.jp

Abstract. One-dimensionally periodic structure of plasma density is produced by a 400 kHz capacitively coupled discharge in 15 Pa argon. The maximum density can be increased up to above 10^{10} - 10^{11} cm⁻³ by increasing the rf power. The density ratio between the higher and lower density layers is maintained at about 0.7 in the present configuration. The transmittance of the microwave in the GHz range is measured and simply calculated. The results indicate the presence of the bandgap near about 3 GHz, which originates in the periodic structure.

1. Introduction

Photonic crystals consisting of periodic structures of dielectric materials are well known to have unique characteristics, e.g., a band gap for a specific frequency (wavelength) relating to its lattice constant [1, 2]. Although recent experimental investigation has demonstrated a measurement of a near-field of the light in nano-scale solid crystal [3], the direct measurement of the wave field inside the crystals, which is important and useful for clarification of the detailed physics and for finding a novel phenomenon such as nonlinear effects, has not been reported because of its experimental difficulties.

As plasma charged particles interact with electromagnetic waves and the wave dispersion relation is resultantly different from that in vacuum, the dielectric constant of the plasma medium depends on the plasma parameters. In the simplest plasma with no magnetic field, high frequency electromagnetic waves interact mainly with electrons near the electron plasma frequency. Recently, plasma photonic crystals (PPCs) have been reported experimentally, theoretically, and numerically for the purpose of active control of microwaves and millimeter waves [4, 5, 6, 7, 8, 9]. One of advantages of the PPCs is that the dielectric constant can be controlled by external experimental parameters such as discharge power, gas pressure, and so on. In the previous and undergoing experiments, the PPCs consisting of atmospheric pressure discharge and relatively higher pressure discharges are used for the medium, where the plasma is periodically produced in millimeter scale [4, 5]. Although the medium with different dielectric constant can appear in the gas phase for the case of the PPCs, the direct measurement of the wave field inside the crystals still remains an experimental challenge because the insertion of the diagnosis tool into the crystals perturbs the discharge operation.



More recently, production of centimeter-scale periodic plasma structure in low pressure discharge has been attempted for the direct measurement of the wave field inside the PPCs [10]. In such a configuration, it is expected that the band gap due to the periodic plasma structure appears in the range of GHz frequency; then small wave detectors can be inserted inside the crystals with no disturbance of the discharges. However, the maximum plasma density in the previous experiment using a dc argon discharge is only 10^9 cm^{-3} ; hence the dielectric constant for GHz waves is unchanged from that for the vacuum. In order to perform the PPC experiments for the GHz microwaves in such a low pressure plasmas, the density should be increased up to $10^{10} - 10^{11} \text{ cm}^{-3}$ at least.

In this paper, a one-dimensionally periodic plasma structure is produced by a 400 kHz capacitively coupled discharge and its density is increased up to above 10^{10} cm^{-3} at the rf power of about 400 W. Further, a transmittance of microwaves in the range of GHz frequency is preliminarily measured; the results indicate a presence of a bandgap in a few GHz and compared with a simple model.

2. Experimental Setup

Experiments are performed in a 60-cm-width, 45-cm-height, and 35-cm-depth grounded vacuum chamber shown in Fig. 1(a). The chamber is evacuated to a base pressure of 10^{-3} Pa by a diffusion/rotary pumping system, after that argon gas is introduced from the side port of the chamber and the gas pressure is maintained at 15 Pa. Living and grounded electrodes shown in Fig. 1(b) are installed inside the chamber. The living electrode is an aluminum plate and powered by a 400 kHz rf power supply through an impedance matching circuit. The rf power can be increased up to about 500 W and the net power can be estimated from the forward and reflected rf powers. Rectangular plastic insulators and grounded aluminum shields are mounted on the living electrodes at 3 cm intervals. Another grounded electrode is located at the upper side, 7 cm away from the living electrode. In such a configuration, the discharge can occur through a capacitively-coupled discharge process only in the region with no insulator and grounded shields; then one-dimensionally modulated plasma-density structure can be formed. The x , y , and z axes and the origin point $(x, y, z) = (0, 0, 0)$ of the axes are defined as indicated in Fig. 1.

The axially movable Langmuir probe (LP) is inserted along the z axis at $(x, y) = (0, 3.5 \text{ cm})$ from the side port of the chamber to diagnose the plasma density. The density is estimated from the ion saturation current of the LP with the measured electron temperature of about 2 eV, assuming a Maxwellian electron energy distribution.

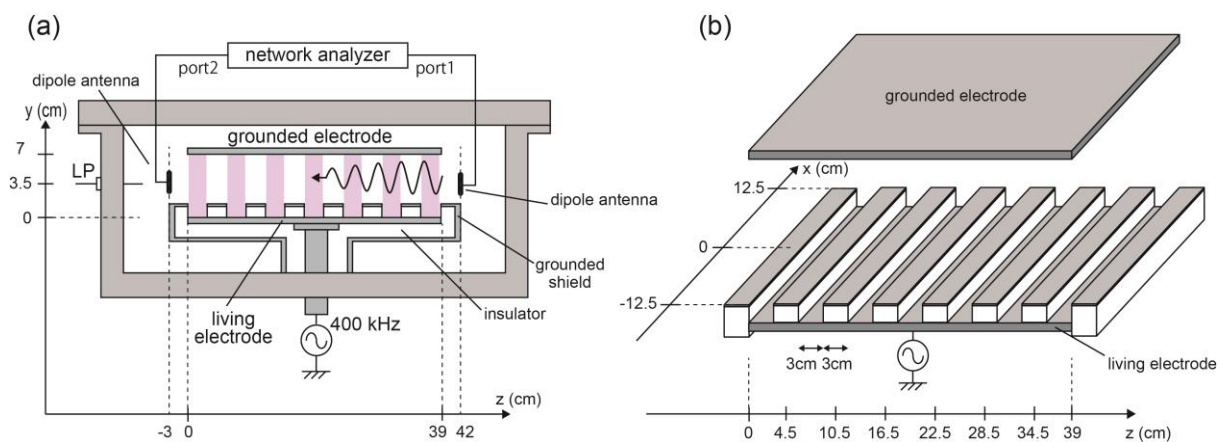


Figure 1. (a) Schematic diagram of the experimental setup. (b) Detailed configuration of the discharge electrodes.

The measurement of a transmittance of microwaves in the range of GHz frequency is performed by two dipole antennas located at $(x, y, z) = (0, 3.5 \text{ cm}, -3 \text{ cm})$ and $(0, 3.5 \text{ cm}, 42 \text{ cm})$, where these antennas have a maximum gain at $\sim 4 \text{ GHz}$. The transmittance coefficient S_{21} between the two antennas including the periodic plasma structure is measured by a network analyzer. To minimize effects of the peripheral chamber wall, electrodes, transmission line, and the antenna characteristic, the transmittance T relating to the plasma structure is defined as

$$T = S_{21 \text{ plasma on}} / S_{21 \text{ plasma off}}, \quad (1)$$

where $S_{21 \text{ plasma on}}$ and $S_{21 \text{ plasma off}}$ are the measured S_{21} with plasma on and off, respectively.

3. Experimental Results

Figure 2 shows the axial profile of the plasma density (open squares) measured by the LP for the net rf power of 180 W, where the solid line is added as a visual guide of the density profile. It is found that the periodic modulation of the plasma density can be formed. The peak positions correspond to the region with no insulators and no grounded shields on the living electrode, while the trough of the density exists in the region with the insulators and grounded shields. As a result, the high density region can be formed at 3 cm intervals, which is dominated by the electrode configuration.

Figure 3(a) shows the plasma densities at the peak ($z = 25.5 \text{ cm}$) and trough ($z = 22.5 \text{ cm}$) positions as a function of the net rf power. The densities in both the regions increases with the increase in the rf power; the maximum density at the peak position is found to be $\sim 8 \times 10^{10} \text{ cm}^{-3}$ at 400 W rf power, which is higher than the previously reported dc discharge [10] by one order of magnitude. Figure 3(b) shows the density ratio of n_{min} at $z = 22.5 \text{ cm}$ (at the trough position) to n_{max} at $z = 25.5 \text{ cm}$ (at the peak position) obtained from Fig. 3(a). The result shows that the density ratio is about 0.7 and is unchanged by the rf power in the present configuration. Hence, it is demonstrated that the one-dimensionally periodic structure of the plasma density of 10^{10} - 10^{11} cm^{-3} is produced by the 400 kHz capacitively coupled discharge, with controlling the absolute value of the maximum density and remaining the density ratio between the peak and trough positions of about 0.7.

The measurement of the transmittance given by Eq. (1) is performed with the rf power as a parameter and the results are plotted in Fig. 4. Transmittances depression less than -20 dB are observed below $\sim 2 \text{ GHz}$. The upper frequency of this transmittance depression seems to increase with an increase in the rf power as indicated by dotted lines in Fig. 4. Further, the transmittance depressions

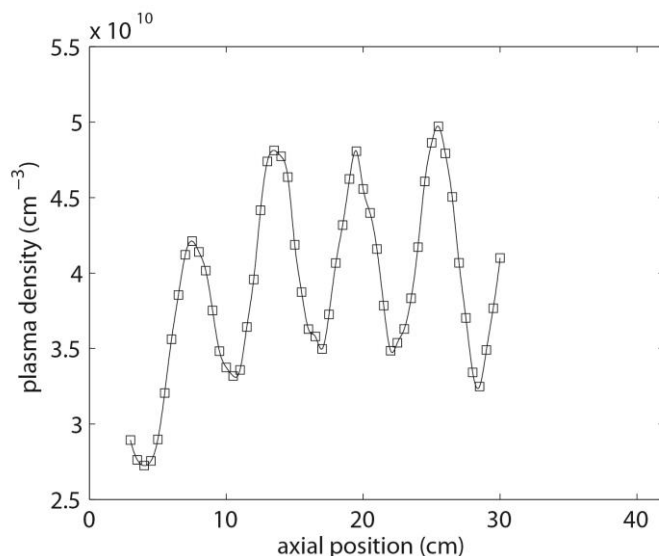


Figure 2. The axial profile of the plasma density measured along z axis and $(x, y) = (0, 3.5 \text{ cm})$ for the net rf power of 180 W (open squares). The solid line is added as a visual guide.

at $\sim 2 - 2.2$ GHz and $\sim 2.5 - 3$ GHz are found to be enhanced by the rf power as indicated by arrows; the frequency of the transmittance depression also seems to be increased by the rf power. Above 3 GHz, it is found that the transmittance is unchanged by the rf power. These changes of the transmittance by the rf power are discussed with a simple model in Sec. 4.

4. Theoretical model

Here an analytical model of the transmittance is described to discuss the experimental results shown in Fig. 4. Now let us consider the simple configuration shown in Fig. 5(a), consisting of the plasma layers with different dielectric constant, which are numbered from 0 to $N + 1$. The forward and reflected waves are labelled as E_i and E_r in the layer 0, and as A_j and B_j in the layer j . The transmitted waves propagating in the layer $N + 1$ is labelled as E_t . Taking account of the boundary conditions between the layer j and $j + 1$, the Maxwell equation gives the relation between these waves as

$$\begin{pmatrix} E_i \\ E_r \end{pmatrix} = M_0 \begin{pmatrix} A_1 \\ B_1 \end{pmatrix}, \quad \begin{pmatrix} A_j \\ B_j \end{pmatrix} = M_j \begin{pmatrix} A_{j+1} \\ B_{j+1} \end{pmatrix}, \quad \begin{pmatrix} A_N \\ B_N \end{pmatrix} = M_N \begin{pmatrix} E_t \\ 0 \end{pmatrix}, \quad (2)$$

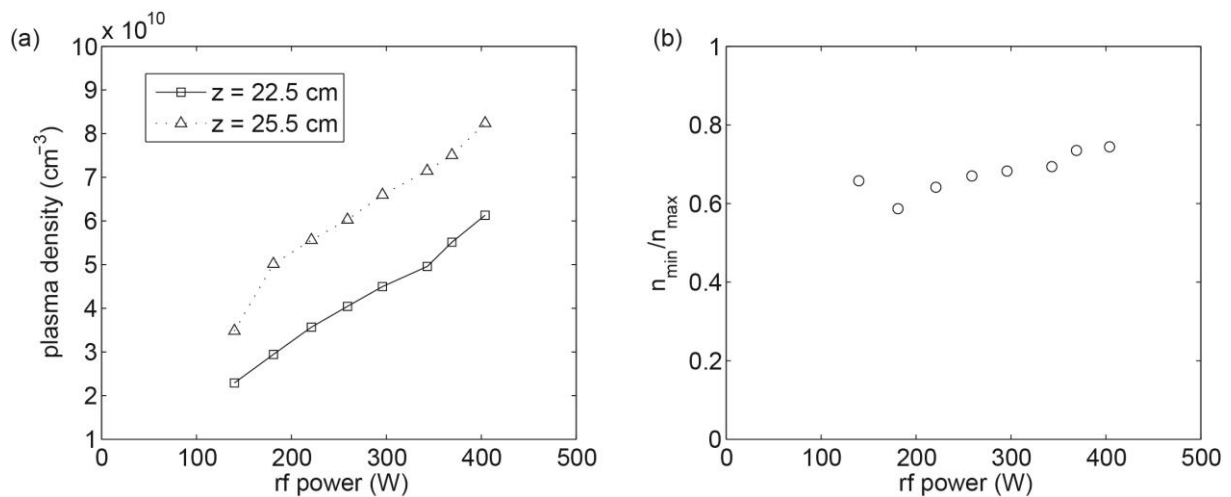


Figure 3. (a) Plasma densities at $z = 22.5$ cm (open squares, n_{\min}) and at $z = 25.5$ cm (open triangles, n_{\max}) corresponding to the peak and trough positions, respectively, versus net rf power. (b) Density ratio $n_{\min} = n_{\max}$ obtained from Fig. 3(a).

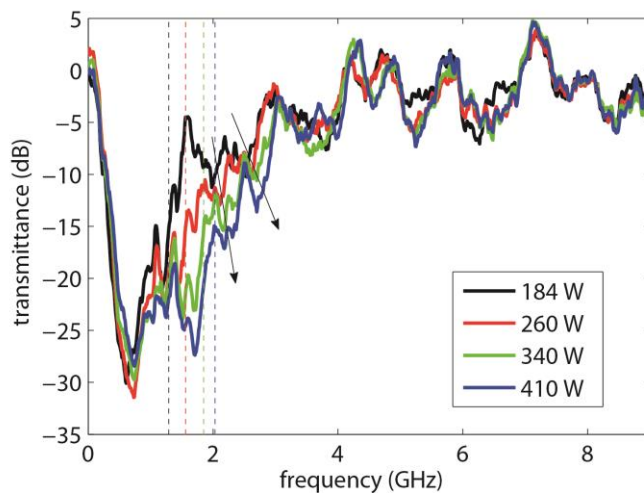


Figure 4. Measured transmittance T for the net rf power of 184 W (black solid line), 260 W (red solid line), 340 W (green solid line), and 410 W (blue solid line), respectively. The dotted lines show the upper frequencies of the transmittance depression below 2 GHz. The arrows indicate that the transmittance depression between 2 GHz and 3 GHz. No change by the rf power is detected above 3 GHz.

position z_j as

$$M_j = \begin{pmatrix} \frac{k_j + k_{j+1}}{2k_j} \exp\{-i(k_j - k_{j+1})z_j\} & \frac{k_j - k_{j+1}}{2k_j} \exp\{-i(k_j + k_{j+1})z_j\} \\ \frac{k_j - k_{j+1}}{2k_j} \exp\{i(k_j + k_{j+1})z_j\} & \frac{k_j + k_{j+1}}{2k_j} \exp\{i(k_j - k_{j+1})z_j\} \end{pmatrix}. \quad (3)$$

Equation (2) and (3) can be rewritten as

$$\begin{pmatrix} E_i \\ E_r \end{pmatrix} = M \begin{pmatrix} E_t \\ 0 \end{pmatrix}, \quad (4)$$

$$\text{where } M \equiv M_0 M_1 M_2 \cdots M_N = \begin{pmatrix} M_{11} & M_{12} \\ M_{21} & M_{22} \end{pmatrix}. \quad (5)$$

The transmittance can be calculated from the above equations as $T = |E_t / E_i|^2 = |1 / M_{11}|^2$. In plasma medium, the dispersion relation of the electromagnetic waves gives the local wave number as $k = (\omega / c) \{1 - (\omega_{pe} / \omega)^2\}^{1/2}$, where $\omega_{pe} = (e^2 n_p / \epsilon_0 m_e)^{1/2}$ is the electron plasma frequency relating to the plasma density.

In the present model, the lower and higher density layers are mutually set at 3 cm intervals to compare with the experiments, where the density is assumed to be uniform in each layer. The density ratio of $n_{min} = n_{max} = 0.7$ is used according to Fig. 3(b), the number of the layers is chosen as $N = 13$, and the layers labeled by even and odd numbers are set as the lower and higher density layers, respectively. The higher density n_{max} is chosen as a parameter to compare with Fig. 4.

Figure 5(b) shows the calculated transmittance with the plasma density n_{max} in the high density layer as a parameter, whose densities correspond to that for the case of each rf power in Fig. 4. Around 2 GHz, a large depression of the transmittance is found to exist, which is close to the electron plasma

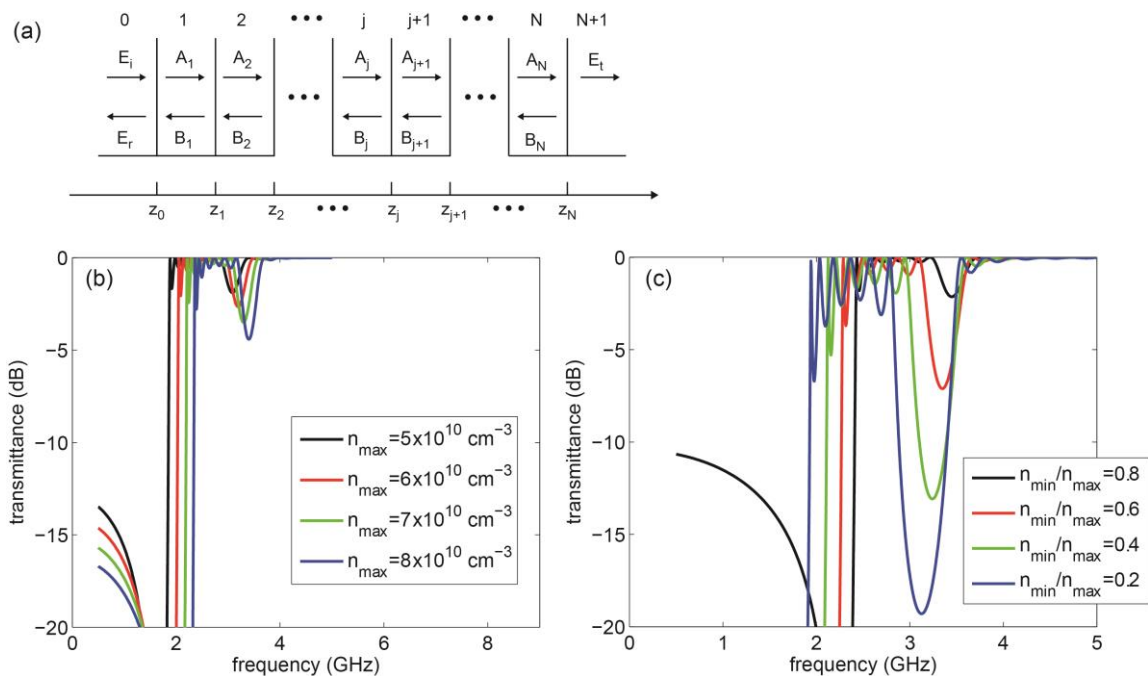


Figure 5. (a) Schematic diagram of the analytical model. (b) Calculated transmittance with the maximum density n_{max} as a parameter, where the density ratio is maintained at $n_{min} / n_{max} = 0.7$. (c) Calculated transmittance with the density ratio n_{min} / n_{max} as a parameter, where the maximum density is maintained at $n_{max} = 8 \times 10^{10} \text{ cm}^{-3}$.

frequency for each density and is similar to the depression indicated by the dotted lines below ~2 GHz in Fig. 4. Furthermore, a small depression appears around 3 GHz in Fig. 5(b); the frequency at this depression also shifts to the high frequency side with the increase in the plasma density. It is confirmed that this depression is due to the periodic structure of the plasma density by calculation with no periodic structure (not shown here); the behavior of the transmittance depression qualitatively agrees with the results in Fig. 4, although only the single depression is observed at about 3 GHz in the calculation, respectively. As the wave does not propagate along z axis exactly in the experiment because of the boundary condition of the chamber wall and the electrodes, some propagation modes are considered to be superimposed. In addition, there might be a density gradient along the x axis, which has not been measured yet due to the absence of a vacuum port. In such a situation, the microwaves will diverge and change their propagation direction. These might be a reason why the two depressions at the different frequencies are detected in Fig. 4. The measurements of the detailed density profile and the microwave and integrating the measured density profile into the analytical and/or numerical calculations of the wave propagation are required in near future. Above 3.5 GHz in Fig. 5, no depression is observed as well as the experimental result in Fig. 4. Based on the above discussion, we can deduce that the experimentally observed depression of the transmittance originates in the one-dimensionally periodic plasma-density modulation shown in Fig. 2.

Moreover, the effect of the density ratio $n_{min} = n_{max}$ is calculated and plotted in Fig. 5(c), where the maximum density is chosen as $n_{max} = 8 \times 10^{10} \text{ cm}^{-3}$. It is clearly found that the transmittance depression can be enhanced by the large density ratio, i.e., large density modulation. Hence it would be better to have a larger density ratio for further PPCs experiments. The production of such profile, the direct measurement of the wave field inside the PPCs, and finding a novel nonlinear phenomenon still remain further subjects.

5. Conclusion

The plasma density of 10^{10} - 10^{11} cm^{-3} is spatially and periodically modulated in centimeter scale by mounting rf shield on a living electrode. The measured and calculated transmittances of the microwave suppose the presence of the bandgap for the microwave range at about 3 GHz. The calculated result also shows that the bandgap can be enhanced by increasing the density ratio between the lower and higher density layers.

Acknowledgement

The authors would like to thank H. Chiba for his technical help for the construction of the chamber. This work is partially supported by a Challenging Exploratory Research (23654197) from MEXT in Japan.

References

- [1] John S, 1987 *Phys. Rev. Lett.* **58** 2486.
- [2] Yablonovitch E, 1987 *Phys. Rev. Lett.* **58** 2059.
- [3] Burrelli M, Engelen R J P, Opheij A, Oosten D van, Mori D, Baba T and Kuipers L, 2009 *Phys. Rev. Lett.* **102** 033902.
- [4] Sakai O, Sakaguchi T and Tachibana K, 2005 *Appl. Phys. Lett.* **87** 241505.
- [5] Sakai O and Tachibana K, 2007 *IEEE Trans. Plasma Sci.* **35** 1267.
- [6] Sakai O, Sakaguchi T and Tachibana K, 2007 *J. Appl. Phys.* **101** 073304.
- [7] Guo B, 2009 *Phys. Plasmas* **16** 043508.
- [8] Fan W, Zhang X and Dong L, 2010 *Phys. Plasmas* **17** 113501.
- [9] Sakai O, Naito T and Tachibana K, 2010 *Phys. Plasmas* **17** 057102.
- [10] Takahashi K, Terui T, Chiba H and Fujiwara T, 2011 *IEEE Trans. Plasma Sci.* **39** 2504.